

Case Report

Comparative evaluation of an advanced electrocoagulation treatment system versus a conventional lime softening treatment for removing Ca^{2+} , SO_4^{2-} , and Mn in groundwater

Jonathan I. Mendez-Ruiz^a, Angie N. Medina-Toala^a, Leonardo Gutierrez^{a,b,c}, Priscila E. Valverde-Armas^{a,*}

^a Escuela Superior Politécnica del Litoral, ESPOL Polytechnic University, Faculty of Engineering in Earth Sciences (FICT), Campus Gustavo Galindo Km. 30.5 Vía Perimetral, Guayaquil, P.O. Box 09-01-5863, Ecuador

^b Centre for Advanced Process Technology for Urban Resource Recovery (CAPTURE), Particle and Interfacial Technology Group, Ghent University, Frieda Saeystraat 1, 9052, Ghent, Belgium

^c Palnt, Particle and Interfacial Technology Group, Department of Green Chemistry and Technology, Faculty of Bioscience Engineering, Ghent University, Coupure Links 653, 9000, Belgium



ARTICLE INFO

Keywords:

Electrochemical process
Alum coagulation
Chemical precipitation
Sustainability
Vulnerable communities

ABSTRACT

This research aims to evaluate the feasibility of a laboratory-scale batch electrocoagulation system for removing hardness, SO_4^{2-} , and manganese from groundwater in San Cristobal, a rural community in the Austro region of Ecuador. The efficiency of the electrocoagulation process was compared to the conventional chemical precipitation with lime and alum coagulation. Various variables were analyzed to evaluate the performance of the electrocoagulation system, including initial pH, operating time, current density, and lime addition. The results showed that a basic environment (\sim pH 8.5) proved more effective in removing hardness and SO_4^{2-} electrolytes by producing ferric flocs with high adsorption properties. Achieving reasonable removal efficiencies for hardness and SO_4^{2-} under neutral or alkaline solution required a minimum of 80 min. Increasing the current density enhanced the removal of hardness and sulfate, and the addition of small amounts of lime (125 mg L^{-1}) increased the hardness removal efficiency from approximately 35 to 50.5%. Under the operating conditions of pH 8.5, 80 min of operation, a current density of 1.0 mA cm^{-2} , and a lime concentration of 75 mg L^{-1} , the system achieved a removal efficiency of 37.6% for hardness, 14.7% for SO_4^{2-} , and a 65.3% for manganese to comply with Ecuadorian drinking water criteria. While lime precipitation and alum coagulation reduced hardness to meet the Ecuadorian INEN 1108 Regulation requirements, the significant demand for treatment chemicals to reduce hardness content rendered the process unsustainable for implementation in the San Cristobal treatment plant. The conventional treatment method failed to reduce sulfate or manganese, and the excessive chemical consumption was not economically viable (1 kg of lime and 0.02 kg of alum per cubic meter of water). In conclusion, this study demonstrates that electrocoagulation, as a chemical-free system, minimizes the use of chemical additives to provide safe water to the population of San Cristobal.

1. Introduction

Each year, an alarming 1.5 million diseases occur due to illnesses related to poor access to clean water, sanitation, and hygiene [1]. The presence of high concentrations of hardness, sulfates, and manganese in water has been linked to various health issues, such as cardiovascular disorders [2], gastrointestinal matters [3,4], and neurological complications [5,6]. This situation not only affects the well-being of individuals

but also burdens peri-urban settlements with economic losses due to the low productivity of the population. Furthermore, the lack of drinking water supply hinders the development of other economic activities in these areas [1,7]. Overcoming water treatment challenges in rural communities remains an urgent issue. Conventional treatment processes have proven ineffective when not operated or maintained correctly. At the same time, advanced technologies have been tested on a limited basis in rural zones [8,9]. Thus, evaluating both conventional and

* Corresponding author.

E-mail address: priesval@espol.edu.ec (P.E. Valverde-Armas).

<https://doi.org/10.1016/j.csee.2023.100448>

Received 17 July 2023; Received in revised form 7 August 2023; Accepted 8 August 2023

Available online 13 August 2023

2666-0164/© 2023 The Authors. Published by Elsevier Ltd. This is an open access article under the CC BY-NC-ND license (<http://creativecommons.org/licenses/by-nc-nd/4.0/>).

non-conventional water treatment technologies is crucial to determine their feasibility in ensuring water quality under the constraints of remote locations.

Traditionally, lime softening has been employed to address water hardness issues, demonstrating removal efficiencies of hardness species exceeding 80% [10,11]. This method, widely adopted for over two centuries, involves the introduction of the chemical base $\text{Ca}(\text{OH})_2$ to disrupt the ionic balance of dissolved substances in water [12]. Lime softening offers ease of operation and low capital cost; however, it is associated with high operating costs due to expenses related to sludge disposal and pH adjustments [13]. Lime softening has proven effective in achieving removal efficiencies from 92 to 100% when pH is alkaline, e.g., around 11 [14], 91% [11,15]. Nevertheless, the availability and affordability of $\text{Ca}(\text{OH})_2$ may vary by region. Also, it is important to note that other contaminants can adversely affect the precipitation reaction. For instance, the presence of sulfate ions promotes the formation of calcium sulfate, leading to increased sludge production [12]. Considering these limitations, advanced technologies offer promising solutions. Electrocoagulation, for instance, is a chemical-free process that minimizes the need for chemical additives, and its operation can be configured for optimal performance under reasonable operating conditions and simple maintenance requirements.

Electrocoagulation is an electrochemical process that involves electrodes connected to a power source within an electrochemical cell, generating coagulants in situ [16,17]. The method comprises three steps: (1) electrolytic oxidation at the anode, which incorporates Fe^{2+} , Fe^{3+} ions, and $\text{O}_{2(g)}$ in the solution; (2) water molecule hydrolysis at the cathode, producing $\text{H}_{2(g)}$ bubbles, and reacting OH^- ions with metal ions to form the coagulant, (3) contaminants adhering to the coagulant and floating to the surface for removal through sedimentation [18]. Compared to traditional chemical precipitation, electrocoagulation offers several advantages. For example, in situ hydroxides as coagulants exhibit adsorption performance 100 times higher than precipitated metallic hydroxides [16]. The air bubbles generated during electrolysis contribute to flotation, resulting in lower sludge production that is easily dehydratable and removing smaller particles than colloids [16,19]. Moreover, the acquisition cost of chemical additives can be significantly reduced, as demonstrated by a wastewater company that achieved a 90% cost reduction by replacing conventional coagulation with electrocoagulation [17]. Various studies, including Rodríguez et al. [20], Bayramoglu et al. [21], Khaled et al. [22], and Espinoza et al. [23] have reported cost reductions of two to threefold when electrocoagulation is deployed instead of chemical coagulation due to the decrease in chemical usage. Bayramoglu et al. [21] found that iron and aluminum electrodes were cost-efficient in comparison to conventional coagulation using ferric or aluminum salts, i.e., costs were below 0.40 USD per m^3 for electrocoagulation compared to a range of 0.70–0.96 USD per m^3 for conventional coagulation. However, it is important to consider the main disadvantages associated with electrocoagulation, such as the cost of electricity in certain rural regions, the need for periodic replacement of sacrificial anodes, and cathode passivation. Consequently, research has explored alternative approaches, including solar-powered electrocoagulation systems deployed in Greece [24], India [25], and Malaysia [26]. In South Africa, recycled corrugated iron has been proposed, achieving 99% sulfate removal efficiency [27]. Furthermore, suggestions have been made for current inversion to enhance electrode dissolution efficiency [28,29].

Laboratory-scale evaluations of electrocoagulation commonly involve the preparation of synthetic samples with varying concentrations of calcium chloride [30,31]. However, it is crucial to recognize that the system's performance under real conditions may differ because natural waters' physicochemical quality may vary significantly. For instance, Halpegama et al. [30] observed a 20% difference in hardness removal efficiency between an electrocoagulation process conducted on a groundwater sample (63%) compared to a synthetic solution (83%). These respective removal percentages were achieved within 52 and 28

min. The authors attributed this difference to the absence of SO_4^{2-} , and Cl^- ions in the synthetic water, which affected the removal efficiency due to changes in solution electronegativity caused by the presence of anions or alterations in positively charged sites within metal hydroxide precipitates.

Consequently, it is essential to conduct studies using synthetic samples that closely resemble the chemical characteristics of natural water to assess removal efficiencies and quantify differences accurately. Another parameter of interest is the material of electrodes, with the literature primarily reporting the use of aluminum electrodes, which yield hardness removal efficiencies of approximately 80% [32,33]. However, Mahmood et al. [31] compared the use of iron and aluminum electrodes with direct current and polarity reversals and found that iron electrodes resulted in 10% higher efficiencies in calcium removal. The underlying reason for this higher reduction has not yet been determined. Furthermore, there is limited information regarding the influence of pH variations on calcium hardness removal. Some authors suggested that adjustments are unnecessary within a pH range of 6.5–7 to remove hardness [38]; however, no experimental evidence was provided. Conversely, other authors propose that the characteristics of floc formed depend on the condition of the medium and that higher pH values can lead to hardness precipitation around the cathode [34]. $\text{Fe}(\text{OH})_3$ can also form in alkaline environments leading to increased flocs generation and the entrapment of more carbonate salts [35]. Overall, there is a lack of systematic experimental studies on Ca^{2+} removal in the literature [35, 36].

Electrocoagulation has also been applied to reduce manganese concentrations. However, removal percentages higher than 70% have typically been achieved through assisted processes, such as agitation, aeration, or electrode modifications. For instance, bench-scale tests conducted by Hanay et al. [37], Al Aji et al. [38], and Gatsios et al. [39] utilized approximately 500–750 mL of water samples, pH values above 6, current densities ranging from 14 to 25 mA cm^{-2} , and constant mixing at 150–200 rpm, with treatment times ranging from 35 to 90 min. These authors explained that the high manganese removal percentages of 85%, 73%, and 89%, respectively, were attributed to cathodic metal deposition, precipitation and co-precipitation mechanisms, sorption capacity of polymeric hydroxides, and the electrochemical stability of manganese as indicated by the Pourbaix diagram within the pH range of 7.5–13. However, no specific explanations were provided regarding the influence of the mixing mechanism. Shafaei et al. [40] evaluated manganese removal within a concentration range of 25–400 mg L^{-1} in a reactor equipped with an incorporated aeration system. The researchers observed that the removal efficiency decreased as the initial manganese concentration increased, possibly because the amount of hydroxide generated was unaffected by the initial concentration. The researchers also investigated manganese removal in a simple electrocoagulation reactor and achieved 100% removal efficiency within 30 min. However, when treating wastewater samples under the same conditions, electrocoagulation only removed 40% of manganese with an operating time of 60 min [41]. The researchers concluded that this behavior could be attributed to the presence of organic material that aluminum hydroxides could adsorb. Mohd et al. [42] modified the electrodes with biochar and achieved 99.9% removal of manganese as Mn^{2+} from a contaminated superficial water sample. The author attributed this high removal efficiency to the adsorption properties of the material.

Since 2016, investigations have been conducted in Ecuador to examine the efficiency of the electrocoagulation process in treating wastewater from the textile and dairy industries [43,44]. However, these studies have primarily focused on removing color and organic substances. For instance, Guamán et al. [44] constructed a laboratory-scale continuous cycle reactor with a capacity of 20 L, consisting of five sub-cells, each containing ten electrodes. The author evaluated the color removal after each compartment by varying the current intensity between 10 and 50A, reducing 66% after the first cell and 96% after the third. In contrast, López et al. [43] evaluated a 9 L

electrocoagulation system, experimenting with various parameters, such as reaction time (30–60 min), number of plates (6 and 12), and voltage (6 and 12 V). The study achieved efficiencies of 93% for chemical oxygen demand, 82% for biochemical oxygen demand, and 76% for suspended solids. However, there is still a need to optimize the range of current intensity to achieve the desired removal efficiencies and to evaluate the impact of other variables such as initial pH, operation time, and minimizing energy requirement. Additionally, it is important to consider the simultaneous removal of various contaminants. This research aims to develop a simple monopolar electrocoagulation system with iron electrodes to remove hardness, Mn^{2+} , and SO_4^{2-} from groundwater, making it suitable for human consumption. The pH conditions will be systematically evaluated under acidic, basic, and neutral conditions. The applied current density will be tested within the 0.3–5.0 $mA\ cm^{-2}$ range, and reaction times will vary from 20 to 140 min. Furthermore, the electrocoagulation operating conditions will be optimized at the laboratory level to ensure the technology's viability in rural communities when scaled up.

2. Materials and methods

2.1. Description of the case study

San Cristobal is located in the northeast region of Azuay province, Ecuador. Due to the lack of surface water bodies and low rainfall with annual precipitation of 500 mm, the terrain is arid. The sector has a predominantly cold climate with mean annual temperatures ranging from 12 to 20 °C. San Cristóbal is favored by microclimates that provide economic growth for the industry in agricultural and livestock activities and the contributions of extractive activities, such as forestry. Fig. 1 shows the study area and zones of economic activities that are conducted.

In 2022, the population of San Cristóbal, comprising La Victoria, Bellavista, Pueblo Nuevo, El Descanso, Cristo Rey, Gauchún, and Pampa Negra, was approximately 2875 citizens [45]. These communities rely on groundwater sourced from a 90-m-deep Loyola Formation aquifer, pumped to the catchment station, and conveyed to the treatment facility in "El Descanso". The plant performs conventional treatment processes to remove the colloidal suspension and hardness and inactivate

microbiological organisms in the water. However, technical and maintenance problems with the treatment units, such as corrosion in the metallic elements of the purification systems, deterioration of the reinforcing steel coating in the treatment unit, useless hardness removal due to cationic exchange softener, and failed pumps, have caused some processes to stop indefinitely, resulting in the distribution of untreated water to the population [9].

2.2. Water sampling

The sampling campaign during the dry season of November 2022 followed the procedures for sampling, handling, and conserving water samples established in the Ecuadorian Technical Guideline INEN 2169 [46]. Groundwater samples ($V=170\ L$) used for the experiments were collected at the inlet flow of the El Descanso water treatment plant using polypropylene containers. The containers were refrigerated, and the water samples were transported in portable coolers, maintaining a temperature between 0 and 5 °C, to ensure the preservation of water quality for further analysis. To assure the reliability and reproducibility of measurements, each water parameter analysis was performed three times, where errors were below 4%.

2.3. Physicochemical analyses

Measurements of the physicochemical properties of water, such as turbidity (TU, NTU), pH, electrical conductivity (EC, $\mu S\ cm^{-1}$), and temperature (T, °C), were performed using a turbidity meter (2100Q, HACH) and a multiparameter (HQ40d, HACH). The turbidity meter was calibrated using formazin standard solutions of 20, 100, and 800 NTU, and the calibration process was validated against a formazin standard solution of 10 NTU. Similarly, the multiparameter sensors were calibrated against standard buffer solutions and a standard conductivity solution, such as 1000 $\mu S\ cm^{-1}$ NaCl, to ensure accurate measurements.

Primary ions, such as water hardness and bicarbonate, were measured by titration methods. In contrast, ions, such as sulfate and chloride, were measured by ultraviolet-visible (UV-Vis) spectrophotometry. Manganese content was measured by chromatography techniques.

The calcium hardness concentration was measured using the burette

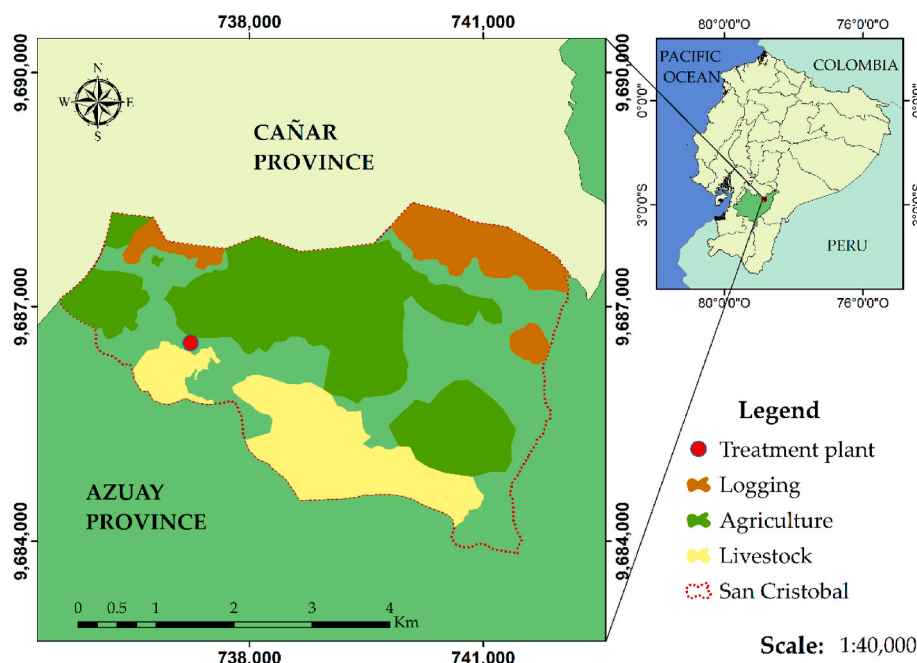


Fig. 1. Study area: San Cristobal community, including the sector where the main economic activities of the zone are carried out.

titration method [47] with ethylenediaminetetraacetic acid (EDTA). Similarly, the total hardness content was measured using an EDTA titrimetric method [48]. These methods determine hardness concentrations between 0 and 25,000 mg L⁻¹ as CaCO₃. The bicarbonate concentration was determined using a volumetric analysis [49] with a standard 0.02 N sulfuric acid solution at the titration end-point. This method measures alkalinity ranging from 0 to 5000 mg L⁻¹ as CaCO₃. The sulfate concentration was measured using the USEPA SulfaVer 4 method [50] with a spectrophotometer (DR 3900, HACH). Since this method measures sulfate content ranging from 2 to 70 mg L⁻¹ SO₄²⁻, higher concentrations were diluted ten times using deionized water before measurement. The spectrophotometer instrument was calibrated using a standard solution of 70 mg L⁻¹ SO₄²⁻. The mercuric thiocyanate method estimated the chloride ion concentration [51]. This method calculates chloride content from 0.10 to 25.00 mg L⁻¹ Cl⁻. The spectrophotometer was calibrated using a standard solution of 20 mg L⁻¹ Cl⁻ prior to measurement. Manganese (Mn) concentrations were measured using inductively coupled plasma optical emission spectroscopy.

2.4. Experimental conditions

Fig. 2 shows the workflow of the experimentation stages, starting with the conventional treatment process of chemical precipitation. The chemical precipitation process included lime precipitation, lime precipitation followed by alum coagulation, and the simultaneous lime precipitation and alum coagulation processes to remove hardness and sulfates. In all experiments, the groundwater samples from San Cristobal were used to evaluate the feasibility of this technology in the community. The second stage consisted of performing the electrocoagulation process by studying the influence of various operating conditions on the system's performance.

2.4.1. Chemical precipitation

Conventional precipitation processes, e.g., lime softening and alum coagulation, were evaluated to remove total and calcium hardness. Lime softening and alum coagulation trials were performed using a four-paddle jar test apparatus (7790 PB-950, Phipps & Birds). The jar test equipment stirred the solution rapidly at 100 rpm for 1 min, followed by gentle stirring at 35 rpm for 20 min. The floc sedimentation time was set at 20 min before measuring the quality properties of the supernatant (softened water).

Hydrated lime (lime) of technical grade was used to prepare the calcium hydroxide stock solution at a concentration of 20 wt%. The coagulant solution was prepared by dissolving 5 g of aluminum sulfate pentahydrate (alum) in 500 mL of deionized water, resulting in a

concentration of 0.02 M. These chemicals were prepared fresh for each experiment. Experiments were conducted three times to ensure reproducibility.

2.4.2. Electrocoagulation

Electrocoagulation experiments were conducted in a batch setting using a 150 mL electrochemical cell. The two-iron electrode configuration was used as the anode and cathode ($A=7.9 \text{ cm}^2$), with an inter-electrode distance of 2.0 cm, as illustrated in Fig. 3. The power supply was a potentiostat/galvanostat (CS150, CorrTest) with a CS Studio5 software interface to adjust experimental configurations, such as applied current densities, and reaction times. Before each experiment, the electrode rods were polished with 2400-grit sandpaper and rinsed with deionized water. Experiments were conducted three times to ensure reproducibility.

a. Effect of reaction time, pH adjustment, current density, and lime addition

The effect of pH and reaction time on contaminant removal efficiency was assessed under galvanostatic conditions. The applied current density remained fixed at 1.5 mA cm⁻² in each experiment. The experiments were carried out in acidic (pH 2.7 ± 0.4), neutral (pH 7.2 ± 0.3), and basic (pH 8.5 ± 0.1) media. The pH was adjusted with 0.02 M HNO₃ or 0.01 M KOH. The reaction time was evaluated from 20 to 220 min.

Current densities from 0.3 to 5.0 mA cm⁻² were tested to remove contaminants, increasing by approximately 0.3 mA cm⁻² each time. In each experiment, the pH was adjusted to a basic medium (pH 8.5 ± 0.1); meanwhile, the electrocoagulation reaction time was adjusted to 80 min.

The effect of lime addition on the contaminant removal with electrocoagulation was evaluated from 25 to 400 mg L⁻¹ lime. In each experiment, the initial pH was adjusted to a basic environment (pH 8.5 ± 0.1); meanwhile, the electrolysis time and current density remained at 80 min and 1.5 mA cm⁻², respectively.

b. Optimization of the Electrocoagulation System

Current density and lime dose variables were studied to minimize energy requirements and treatment chemicals on a bench-lab scale. The selected current density values ranged from 1.0 to 1.8 mA cm⁻², and the added lime doses ranged from 25 to 125 mg L⁻¹. In each experiment, the initial pH was adjusted to a basic medium (pH 8.5 ± 0.1), and the reaction time remained at 80 min.

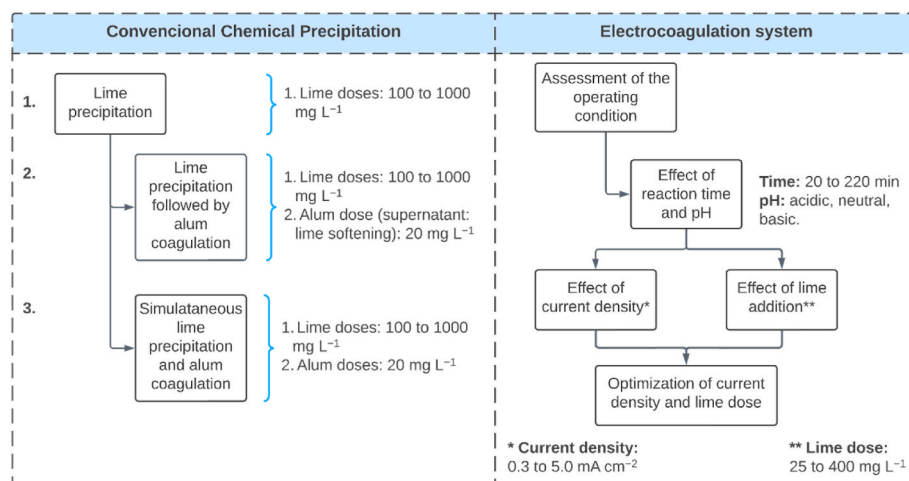


Fig. 2. Schematic of the experimentation methodology.

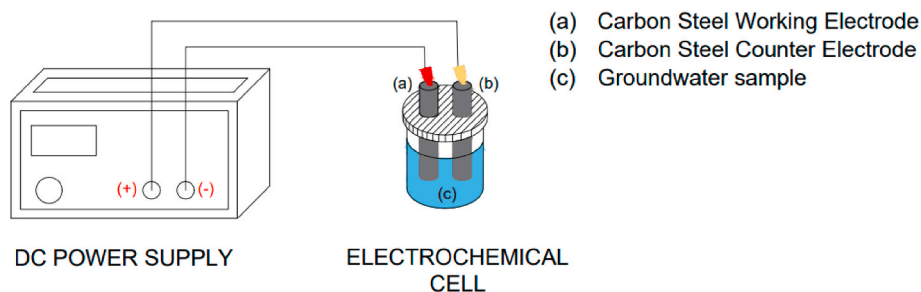


Fig. 3. Schematic of the electrocoagulation system.

3. Results and discussion

3.1. Chemical precipitation

a. Lime softening

Fig. 4 shows the residual concentrations of total hardness, calcium hardness, and bicarbonate during lime precipitation. The addition of lime led to a decrease in total and calcium hardness. For example, the introduction of 1000 mg L^{-1} of lime reduced the total hardness content from $674.0 \pm 4.6 \text{ mg L}^{-1}$ to $228.0 \pm 3.6 \text{ mg L}^{-1}$ as CaCO_3 , resulting in an 89.2% reduction in hardness, as depicted in Fig. 4(a). The results demonstrate that most hardness ions removed during lime precipitation corresponded to soluble calcium compounds. At a lime dose of 1000 mg L^{-1} , the residual concentration of calcium hardness was $50.0 \pm 3.2 \text{ mg L}^{-1}$ as CaCO_3 , as shown in Fig. 4(b). Previous studies by Korchuganova et al. [52], Comstock et al. [53], and Leeuwen et al. [54] have indicated that the sludge composition of lime softening primarily consists of calcium precipitates, such as CaCO_3 and Ca(OH)_2 .

On the other hand, no significant removal of magnesium hardness was observed following lime implementation. The initial concentration of magnesium hardness at $210.0 \pm 2.6 \text{ mg L}^{-1} \text{ CaCO}_3$ remained relatively constant at lime doses between 100 and 400 mg L^{-1} , for instance, at $218.0 \pm 17.1 \text{ mg L}^{-1} \text{ CaCO}_3$. However, doses greater than 500 mg L^{-1} resulted in a significant reduction in bicarbonate concentration from $564.0 \pm 10.2 \text{ mg L}^{-1}$ to $< 304.0 \pm 12.3 \text{ mg L}^{-1}$, leading to an increase in pH from 7.5 ± 0.1 to $> 9.1 \pm 0.3$. This rise in pH influences the abundance of hydroxyl ions, promoting the precipitation of magnesium hydroxide and reducing the concentration of magnesium hardness to $159.0 \pm 24.1 \text{ mg L}^{-1} \text{ CaCO}_3$. This phenomenon has also been reported by Prazeres et al. [55], Chen et al. [56], and Madeira et al. [57], where precipitation of magnesium hydroxide was achieved at pH values > 9 .

The removal of hardness ions through lime precipitation, e.g., calcium and magnesium, resulted in a decrease in electrical conductivity from $1702.0 \pm 56.0 \mu\text{S cm}^{-1}$ to $1203.0 \pm 15.0 \mu\text{S cm}^{-1}$ when 1000 mg L^{-1} of lime was dosed. The presence of bicarbonate facilitated this reduction by promoting the precipitation of calcium salts, mainly in the form of calcium carbonate [58,59]. On the contrary, Zayen et al. [60] reported increased calcium concentration and electrical conductivity once the bicarbonate content was nearly depleted. Unfortunately, lime softening adversely affected residual turbidity in the solution, as illustrated in Fig. 4(c). The colloidal content increased from 18.1 ± 1.9 to $49.8 \pm 1.7 \text{ NTU}$ at 1000 mg L^{-1} . Similar observations of increased residual turbidity resulting from the application of softening chemicals were documented by Yan et al. [61].

b. Lime addition followed by alum coagulation.

The primary drawback of lime softening is the introduction of colloidal matter into the solution, which requires an additional treatment mechanism to eliminate the incorporated turbidity. Alum coagulation followed by lime softening to address this issue and reduce

turbidity. The supernatants obtained from lime softening were coagulated in jar test experiments with 20.0 mg L^{-1} of alum. Subsequently, the turbidity values were reduced to $1.3 \pm 0.2 \text{ NTU}$, representing $\sim 95.0\%$ reduction in the colloidal suspension. Additionally, the pH of the solution increased from 7.5 ± 0.2 to 9.1 ± 0.6 due to the introduction of hydroxide ions during the lime addition. This pH increase creates favorable conditions for the formation of hydroxides, such as aluminum hydroxides, facilitating the destabilization and aggregation of colloidal impurities [62,63].

As expected, coagulation had a minimal impact on the removal of hardness, as depicted in Fig. 5. The efficiency of alum coagulation in removing total hardness was generally below 12.3%. A similar trend was observed in the reduction of soluble calcium compounds, with an efficiency below 5.6% (Fig. 5(b)). These findings are consistent with the results reported by Ghernaout et al. [64]. Bouchahm et al. [65] also reported comparable outcomes, demonstrating low efficiencies of aluminum sulfate coagulation in removing hardness ions, approximately $15.0 \pm 5.0\%$ for total hardness and $8.0 \pm 2.0\%$ for calcium hardness.

One of the key limitations of implementing this in-series process is the requirement for physical space to accommodate two sedimentation ponds for decanting the formed flocs. Moreover, the generation of additional treatment byproducts, namely sludge, would require frequent maintenance protocols to prevent obstructions or degradation of the sludge [66]. This would ultimately increase the costs and complexity associated with maintaining the system.

c. Simultaneous lime precipitation and alum coagulation process

The utilization of treatment chemicals in a single process eliminates the need for sedimentation ponds in series. This section explores the simultaneous removal of hardness and residual turbidity by varying lime concentrations from 100 to 1000 mg L^{-1} while using a fixed coagulant dose of 20 mg L^{-1} of alum.

The combined lime precipitation and alum coagulation process exhibited excellent effectiveness in reducing hardness concentrations, as depicted in Fig. 6. When a simultaneous dosage of 1000 mg L^{-1} of lime and 20 mg L^{-1} of alum was applied, a hardness reduction of approximately 66.5% was achieved. This resulted in a residual calcium hardness of $24.0 \pm 12.6 \text{ mg L}^{-1}$ as CaCO_3 , corresponding to a high removal efficiency of $\sim 94.8\%$. Additionally, the electrical conductivity decreased from 1752 ± 21 to $1206 \pm 45 \mu\text{S cm}^{-1}$. However, it is worth noting that the presence of the alum coagulant hindered the lime precipitation mechanism's effectiveness in removing hardness at low lime doses, a finding also reported by Ghernaout et al. [64]. For lime doses below 400 mg L^{-1} , the concurrent precipitation-coagulation process demonstrated lower effectiveness in removing calcium hardness compared to the sole precipitation with lime, as illustrated in Fig. 6(b). This can be attributed to the influence of the coagulant on the solution's pH [67]. When alum was simultaneously dosed with lime concentrations of up to 400 mg L^{-1} , the pH did not exceed 7.6 ± 0.1 , hindering the reduction of calcium hardness in calcium carbonate flocs [68]. However, increasing lime doses ($>400 \text{ mg L}^{-1}$) compensated for the negative impact of the

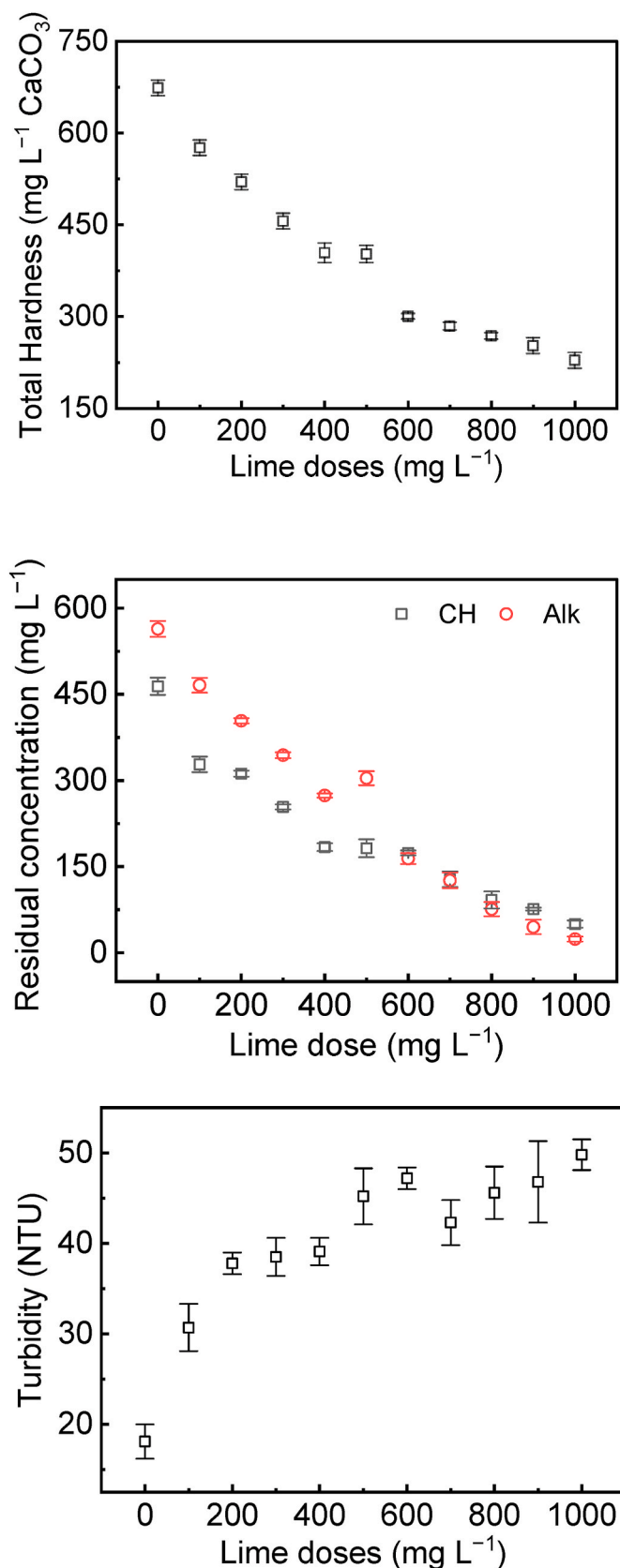


Fig. 4. (a) Total hardness, (b) calcium hardness (CH) and bicarbonate (Alk), and (c) turbidity residual concentrations in supernatant versus lime doses.

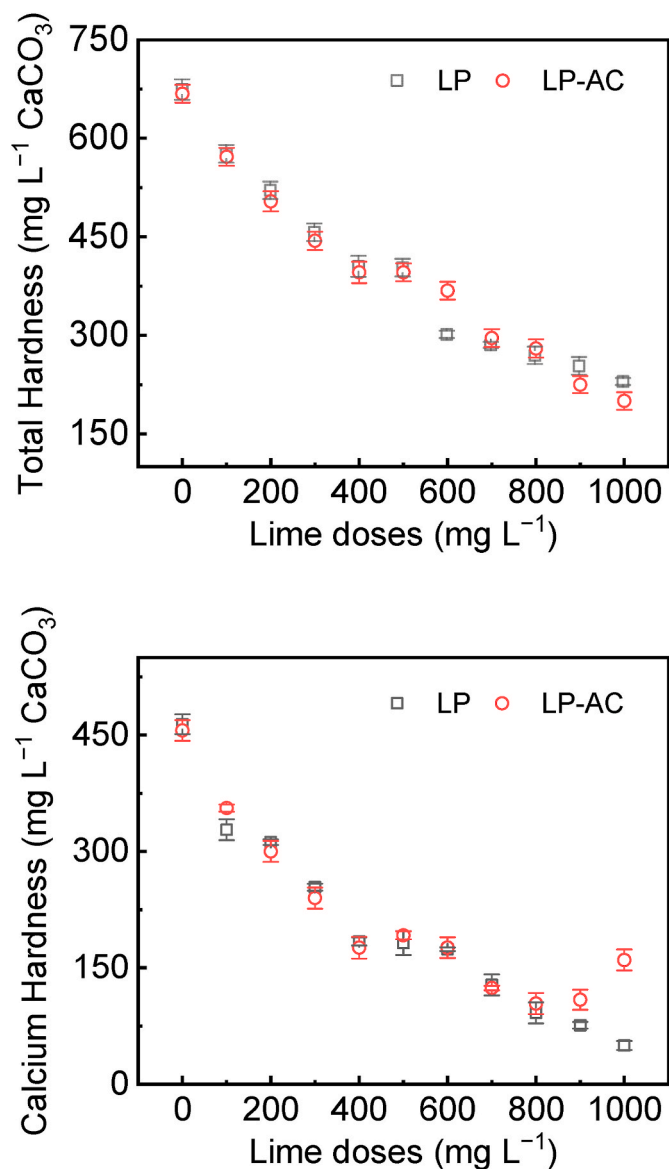


Fig. 5. (a) Total hardness and (b) calcium hardness concentration in the supernatant versus lime dose. Two scenarios: (i) lime precipitation (LP) and (ii) in-series lime precipitation and alum coagulation (LP-AC).

coagulant by promoting the availability of hydroxides in the solution, leading to a higher pH (9.3 ± 0.7). This facilitates the synergistic removal of calcium compounds through the adsorption capacity of aluminum hydroxide and the precipitation process, which converts calcium to calcium carbonates. After the simultaneous precipitation-coagulation process, the residual turbidity remained at 4.3 ± 1.5 NTU.

3.2. Electrocoagulation

3.2.1. Removal efficiency versus operating time in different pH media

Fig. 7 illustrates the results of the electrocoagulation process, using iron rod electrodes, for removing hardness concentrations at various reaction times, ranging from 20 to 220 min. The experiment was conducted under different pH conditions and an applied current density of 1.5 mA cm^{-2} . Fig. 7(a) shows a clear decrease in hardness concentration as the electrocoagulation time increases. The minimum operating time required to achieve reasonable removal efficiencies in neutral and basic solutions was 80 min. For instance, at 80 min of operation, the removal

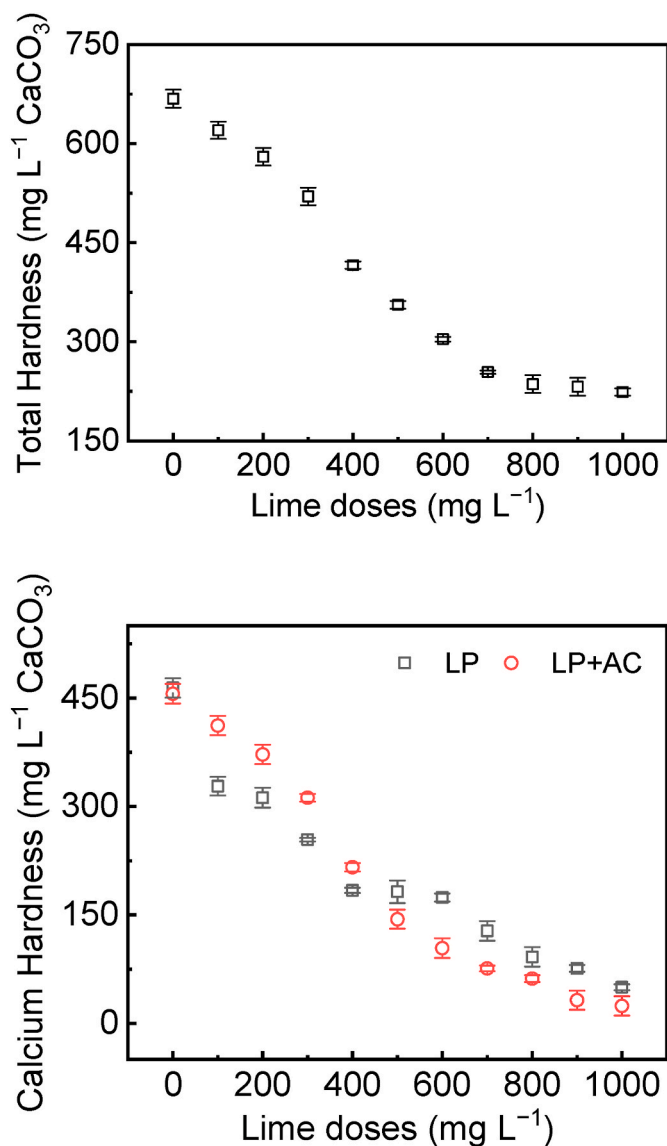


Fig. 6. (a) Total hardness, and (b) calcium hardness concentration in supernatant versus lime doses and a fixed alum dose of 20 mg L⁻¹. Two scenarios were studied in calcium hardness removal: (i) lime precipitation (LP) and (ii) simultaneous process of lime precipitation and alum coagulation process (LP + AC).

efficiencies for hardness were 11.9% and 25.2% for neutral and basic conditions, respectively. By extending the electrocoagulation operating time to 220 min, the reduction in hardness significantly improved, reaching 51.6% for neutral pH and 58.6% for basic pH. Similar improvements in the efficiency of hardness salts removal were reported by Yang [69], Kobya et al. [70], and Malakootian et al. [34] when longer operating times were employed. According to Faraday's law, the duration of operation directly affects the release rate of metal ions during anodic dissolution, leading to increased in-situ coagulant production and higher removal efficiencies [71]. The presence of hydroxyl ions is also crucial for the formation of hydroxide flocs [72]. Consequently, maintaining a basic pH of around 8.5 enhanced the efficiency of hardness removal as the treatment time was extended. In contrast, electrocoagulation proved ineffective in removing hardness under acidic conditions, with efficiencies remaining below 10%, even with prolonged operating times of up to 220 min. This discrepancy in the efficiencies under different pH conditions can be attributed to the characteristics of the hydroxide flocs formed. The metal hydroxide flocs generated in basic

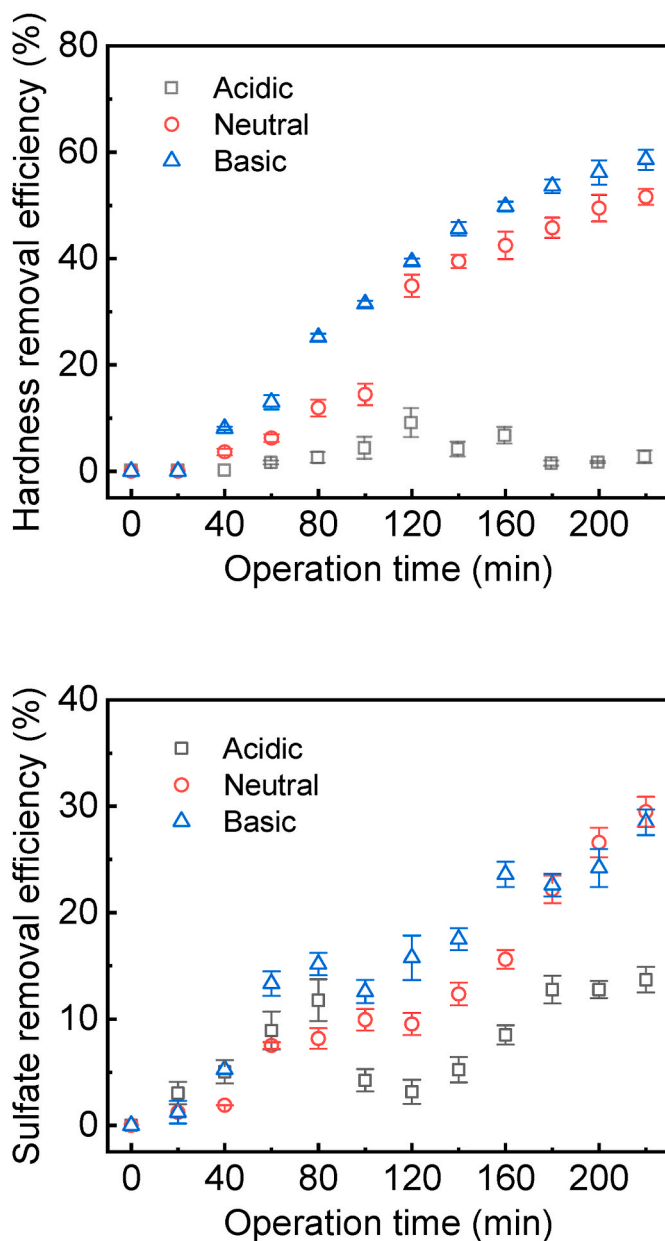


Fig. 7. (a) Total hardness and (b) sulfate removal efficiencies in supernatant versus electrocoagulation operating time in different pH solutions (acidic, neutral, and basic). The applied current density was fixed at 1.5 mA cm⁻².

solutions, such as Fe(OH)_{3(s)}, exhibit a stronger affinity for co-precipitating hardness due to their large surface area compared to the Fe(OH)_{2(s)} flocs produced in acidic solutions [73,74,75].

Fig. 7(b) presents the results of the electrocoagulation process for removing sulfate concentrations from the solution at various electrocoagulation times and pH conditions. The data indicates that neutral and basic solutions yield more favorable results for SO₄²⁻ removal as the operating time increases. Under neutral conditions, the electrocoagulation efficiency for sulfate removal improved from 8.2% to approximately 29.5%, with an increase in treatment time from 80 to 220 min. Similarly, efficiency increased from 15.2% to 28.5% in basic solutions. However, sulfate removal efficiency remained below 15% under acidic conditions, indicating ineffectiveness. Several authors support these findings, with Al-Raad et al. [76] and Yamba et al. [27] reporting higher removal efficiencies under neutral and basic pH conditions, which can be attributed to the presence of hydroxyl ions facilitating the formation of iron flocs. The mechanism behind sulfate removal involves

the adsorption capacity of the positively charged surface of iron hydroxides for anions adsorption.

3.3. Performance of conventional chemical precipitation and electrocoagulation in contaminant removal

Hardness, sulfate, and manganese (Mn) are contaminants in water that pose restrictions on its usage and consumption [77], causing inconveniences for end-users, including health issues and economic losses [78]. To avoid these issues, the Ecuadorian Water Quality Regulation, INEN 1108, sets a maximum hardness threshold of $500 \text{ mg L}^{-1} \text{ CaCO}_3$ for drinking water [79]. On the other hand, sulfate significantly impacts water's taste properties [96]. The permissible sulfate limit in drinking water, according to INEN 1108, is 400 mg L^{-1} [79]. Sulfate concentrations exceeding 500 mg L^{-1} are directly associated with gastrointestinal disorders [80], acute dehydration [81], and interference with nutrient absorption [82]. Manganese in water, when present in concentrations above 0.05 mg L^{-1} , can cause taste issues and stains on plumbing fixtures [83]. The INEN 1108 standard prohibits manganese concentrations beyond 0.4 mg L^{-1} for human consumption [79], as they pose an increased risk of cognitive performance deterioration, neurotoxicity [84], and cardiovascular problems [85]. Given these concerns, deploying effective treatment procedures is mandatory to produce drinking water compliant with sanitary legislation.

Lime precipitation is a widely used treatment process for efficiently removing high hardness levels from water. This process involves raising the pH of the solution, which facilitates the precipitation of hardness in the form of calcium carbonates or magnesium hydroxides [86]. In Section 3.1.c, a simultaneous precipitation-coagulation process was examined, revealing that a combination of 400 mg L^{-1} lime dose and 20 mg L^{-1} of alum effectively reduced hardness concentrations from 668 mg L^{-1} to approximately $416 \text{ mg L}^{-1} \text{ CaCO}_3$ by elevating the pH from 7.1 to around 8.0. This condition ensures compliance with the maximum limits for hardness (500 mg L^{-1}) and turbidity (less than 5 NTU) as established by INEN 1108 [79]. However, it is important to note that meeting the hardness threshold does not guarantee the absence of technical problems. Water with a hardness level exceeding approximately 200 mg L^{-1} can lead to the formation of calcium carbonate crystal deposits in treatment appliances, distribution systems, and water reservoirs within residential facilities. This issue becomes more significant when other chemical characteristics of water, such as pH and alkalinity, come into play [87]. Conversely, water with hardness levels below 100 mg L^{-1} may have a low pH buffering capacity, resulting in corrosive properties [88].

To address these constraints and comply with local drinking water standards for hardness and turbidity, it was determined that lime doses exceeding 800 mg L^{-1} are optimal for precipitating hardness, resulting in a residual hardness concentration of approximately $230 \pm 8 \text{ mg L}^{-1} \text{ CaCO}_3$ at pH levels higher than 9.5. However, the use of such large quantities of chemicals raises concerns regarding cost and chemical usage. For instance, translating 1000 mg L^{-1} of lime and 20 mg L^{-1} of alum into practical amounts would require 1 kg of lime and 0.02 kg of alum to treat 1 m^3 of water. This high demand for chemicals imposes a significant economic burden on San Cristobal, particularly considering the area's limited financial resources, where the local community manages the treatment facility [9]. Furthermore, it is important to note that traditional lime precipitation and alum coagulation impact the water's pH requiring subsequent pH adjustment to a range between 6.5 and 8.5 [79]. Additionally, these processes may not efficiently address sulfate and manganese concentrations in the water, presenting another drawback of this treatment method.

Electrocoagulation is an advanced water treatment technology that offers numerous advantages. One of its key benefits is that it operates as a chemical-free system, eliminating the need for external coagulant agents and reducing reliance on additional chemicals. Moreover, electrocoagulation has proven to be effective in simultaneously removing

multiple contaminants from water, and by optimizing operating variables, it can achieve efficient treatment while reducing energy consumption, making it a robust system and a sustainable solution [89–91]. Section 3.2 discusses the optimal conditions for pH and electrocoagulation operating time. The findings indicate that basic solutions with a pH of approximately 8.5 and an operating time of 80 minutes yield favorable results. Under these conditions, and with an applied fixed current density of 1.5 mA cm^{-2} , the residual concentration of hardness was reduced to $508 \text{ mg L}^{-1} \text{ CaCO}_3$, corresponding to a removal efficiency of 25.2%. Similarly, sulfate was removed to a concentration of 460 mg L^{-1} , with a removal efficiency of 15.2%. However, these concentrations still exceed the thresholds recommended by Ecuadorian water quality regulations.

In order to enhance the removal efficiencies of contaminants, the effect of increasing current densities on the electrocoagulation process was investigated. Current density values ranging from 0.3 to 5.0 mA cm^{-2} were tested, while maintaining an optimal initial pH of 8.5 and an operating time of 80 min as the initial conditions for these experiments. As shown in Fig. 8, it is evident that increasing the current density led to enhanced hardness reduction. Specifically, as the current density increased from 0.3 to 5.0 mA cm^{-2} , the removal efficiency for hardness increased from 23% to approximately 73%, representing a significant enhancement of approximately 50%. Similar observations have been reported in studies conducted by Sefatjoo et al. [33], Malakootian et al. [34], and Zhao et al. [35], where the efficiency of hardness removal improved by 25%, 35%, and 40%, respectively, with increasing current density. This improvement can be attributed to the higher rate of coagulant dose released in the solution, which is directly proportional to the current density [31]. Consequently, larger quantities of $\text{Fe}(\text{OH})_3$ coagulants are available to destabilize and settle more pollutants, including hardness, as sediments [92]. Additionally, Chen [93] reported that higher current densities promote hydrogen evolution from the cathode, forming smaller bubbles. These bubbles possess a larger surface area, facilitating particle attachment and the removal of contaminants through flotation. However, it is worth noting that extremely high current densities and prolonged electrocoagulation operating times can pose challenges in floc separation due to the high density of the resulting precipitates and the poor affinity between hydroxide flocs and gas bubbles in the solution, as observed by Halpegama et al. [30].

Significant reductions in sulfate content were observed with increasing current densities (ranging from 0.3 to 5.0 mA cm^{-2}) during

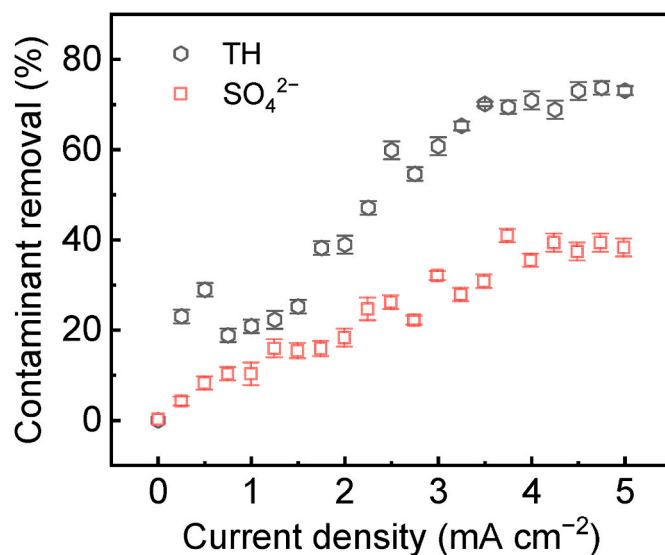


Fig. 8. Total hardness (TH) and sulfate removal efficiencies in the supernatant versus current density during electrocoagulation. The pH and reaction time were fixed to alkaline ($\text{pH } 8.5 \pm 0.1$) and 80 minutes, respectively.

the electrocoagulation process, resulting in removal efficiencies of approximately 40%, as shown in Fig. 8. These findings align with similar studies conducted by Murugananthan et al. [94], Nariyan et al. [95], and Mamelkina et al. [29], which reported sulfate reduction of around 30%, 35%, and 50%, respectively, as the current density increased. The reductions in sulfate can be attributed to the adsorption capacity of the coagulant substances, particularly ferric hydroxides [94,96], as well as the formation of insoluble iron flocs, such as $\text{FeSO}_4(\text{OH})_2$, during anodic dissolution [97–99]. It is important to note that the chemical composition of the water can influence sulfate removal, as other contaminants may kinetically compete with sulfate for co-precipitation with coagulant substances, as reported by Angel et al. [100].

Furthermore, the reduction in hardness species, including calcium and sulfate compounds, during electrocoagulation led to a decrease in electrical conductivity, consistent with the findings achieved by Farhadi et al. [101]. For instance, after applying a current density of 4.4 mA cm^{-2} , the residual electrical conductivity was measured at $1248 \pm 14 \mu\text{S cm}^{-1}$, corresponding to a reduction of approximately 29.8%. However, it was observed that surpassing this current density threshold had a detrimental effect on the electrical conductivity, as evidenced by an increase to $1733 \pm 23 \mu\text{S cm}^{-1}$ at 5.0 mA cm^{-2} .

Fig. 9 presents the impact of lime addition on the efficiency of the electrocoagulation process in reducing hardness and sulfate concentrations. The results clearly indicate that incorporating lime into the electrocoagulation system enhances its effectiveness in removing hardness. As described in Section 3.2, the optimal electrocoagulation conditions, including an alkaline environment with a pH of approximately 8.5, an electrocoagulation time of 80 min, and an applied current density of 1.5 mA cm^{-2} , resulted in a hardness removal of approximately 25.2% and a residual electrical conductivity of $1482 \pm 30 \mu\text{S cm}^{-1}$. However, by introducing 125 mg L^{-1} of lime into the system, the efficiency of hardness removal increased to around 50.5%, and the residual electrical conductivity was measured at $1320 \pm 8 \mu\text{S cm}^{-1}$. These improvements can be attributed to the combined removal mechanisms of hardness co-precipitation on the surface of iron flocs and the formation of CaCO_3 and $\text{Ca}(\text{OH})_2$ deposits, which occur due to the pH elevation caused by lime addition [64]. Nevertheless, it is important to note that lime concentrations exceeding 125 mg L^{-1} showed minimal additional

improvements in efficiency. In contrast, Fig. 9 demonstrates that the introduction of lime did not enhance the electrocoagulation efficiency for sulfate reduction. The sulfate reduction efficiency remained unchanged at approximately 16.4% regardless of the lime dose. This behavior suggests that the sole removal mechanism for sulfate is the adsorption capacity of iron hydroxide flocs generated during the electrocoagulation process, promoting the co-precipitation of negatively charged contaminants [27], without lime addition.

The effect of lime doses on the electrocoagulation process was investigated at a current density of 1.5 mA cm^{-2} . In order to determine the optimal operating conditions for simultaneous reduction of hardness and sulfate concentrations in a single treatment stage, the effect of lime doses was evaluated within different current density values ranging from 1.0 to 1.8 mA cm^{-2} . Throughout the experiments, the initial pH of the solution was maintained at approximately 8.5, and the reaction time was fixed at 80 min.

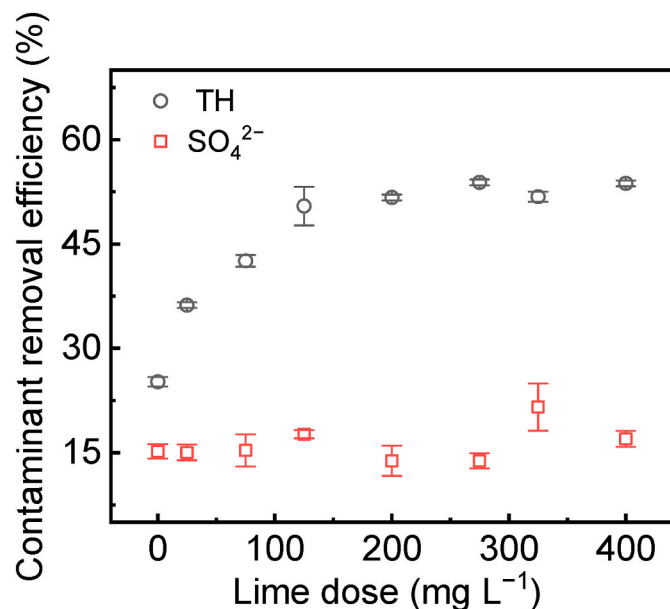


Fig. 9. Total hardness and sulfate removal efficiencies in supernatant versus current density during electrocoagulation. The electrocoagulation parameters, such as pH, current density, and reaction time, were fixed to alkaline ($\text{pH } 8.5 \pm 0.1$), 1.5 mA cm^{-2} , and 80 minutes, respectively.

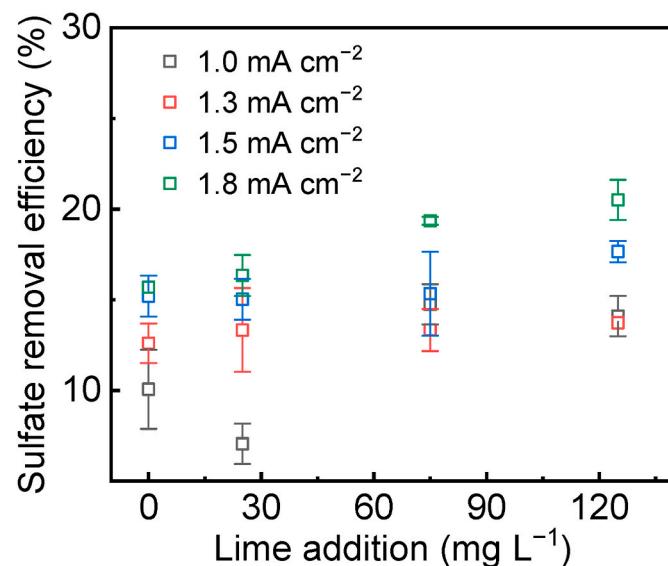
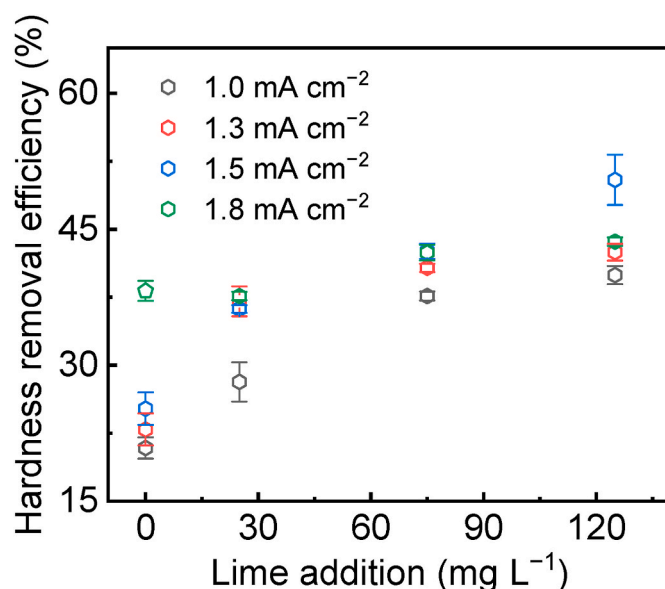


Fig. 10. Total hardness and sulfate removal efficiencies in supernatant versus lime doses at different current densities during electrocoagulation. The electrocoagulation parameters, such as pH and reaction time, were fixed to alkaline ($\text{pH } 8.5 \pm 0.1$), and 80 minutes, respectively.

Fig. 10 illustrates the residual concentrations of hardness and sulfate with increasing lime dose under different current density conditions. As expected, the introduction of lime doses into the electrocoagulation system enhanced the efficiency of hardness removal. Interestingly, the efficiency of hardness reduction remained consistent regardless of the current density applied (ranging from 1.0 to 1.8 mA cm⁻²) when lime was incorporated, as shown in Fig. 10(a). For example, when a small dose of 25 mg L⁻¹ of lime was introduced to electrocoagulation, the efficiency consistently reached approximately 40%, regardless of the applied current density. This trend continued when lime doses from 75 to 125 mg L⁻¹, with the hardness reduction plateauing at around 42%, irrespective of the current density. This finding provides an opportunity to select a lower current density, such as 1.0 mA cm⁻², to minimize potential energy requirements in larger-scale applications while effectively addressing the technical challenges associated with water hardness. It is worth noting that increasing the current density significantly impacts the operating cost of contaminant removal, as evidenced by other studies summarized in Table 1. Furthermore, under these operating conditions, it was observed that the final pH remained below within the drinking water range (pH < 8.5).

Fig. 10(b) presents the residual concentration of sulfate with increasing lime dose under different current densities during electrocoagulation. As anticipated, the addition of lime did not enhance the efficiency of sulfate removal through electrocoagulation. For example, at a current density of 1.0 mA cm⁻² and a lime dose of 75 mg L⁻¹, the system achieved only approximately 15% removal of the initial sulfate content, resulting in a residual concentration of 479.1 mg L⁻¹ SO₄²⁻. Increasing the lime dose to 125 mg L⁻¹ did not improve efficiency, which remained around 15%. This lack of effect on sulfate removal persisted even at higher current densities, such as 1.8 mA cm⁻². Under this current density condition, increasing the lime dose from 75 mg L⁻¹ to 125 mg L⁻¹ did not improve the system efficiency beyond 20%, and the residual concentration remained at 453 mg L⁻¹ SO₄²⁻. The electrocoagulation conditions, including applied current densities ranging from 1.0 to 1.80 mA cm⁻² and lime doses ranging from 25 to 125 mg L⁻¹, did not meet the maximum limit of 400 mg L⁻¹ SO₄²⁻ for drinking water, as specified by Ecuadorian regulations. Nevertheless, these operating conditions can still contribute to a reduction in the incidence of gastrointestinal disorders among end-users, as the Environmental Protection Agency recommends sulfate concentrations below 500 mg L⁻¹ SO₄²⁻ to mitigate such issues [80]. Achieving higher removal efficiencies may require increased energy inputs. For instance, Angel et al. [100] reported a specific energy consumption of 1.92 kWh m⁻³ when applying a current density of 6 mA cm⁻² to achieve 28% removal of SO₄²⁻. Alternatively, some researchers have explored the use of corrugated iron electrodes as a cost-effective and energy-effective option due to their reusability [27].

Manganese removal from the solution was also evaluated during electrocoagulation, using various current density values ranging from 1.0 to 1.8 mA cm⁻². In order to achieve simultaneous removal of manganese, hardness, and sulfate in a single treatment stage, the optimal operating conditions for electrocoagulation were maintained in each experiment. This included a pH of approximately 8.5, an operating time of 80 min, and a lime dose of 75 mg L⁻¹. The results showed that

increasing the current density under basic conditions did not improve manganese removal. The initial manganese concentration in the water, which was 1.18 mg L⁻¹ Mn, was reduced to 0.41 mg L⁻¹, 0.47 mg L⁻¹, and 0.59 mg L⁻¹ when applying current densities of 1.0, 1.3, and 1.8 mA cm⁻², respectively. These values corresponded to 65.3%, 60.2%, and 50% of electrocoagulation efficiencies for manganese removal. In contrast, Shafaei et al. [41], Adhoum et al. [104], and Alkizwini et al. [105] reported improved manganese removal as the current density increased. These authors achieved such efficiencies in synthetic solutions using aluminum anode electrodes and neutral pH ranges. The difference with the results obtained in this study could be attributed to the pH evolution during the electrocoagulation, where the solution pH increases to an alkaline level with higher current density. Shafaei et al. [40] determined that a pH of approximately 7–8 is efficient for precipitating manganese, such as Mn(OH)₂, at the cathode. The pH of the water samples had values around 8.3, 8.6, and 8.9 when applying current densities of 1.0, 1.3, and 1.8 mA cm⁻², respectively, which hindered further manganese removal as the pH increased. However, it is worth noting that the condition with the highest manganese removal efficiency, achieved at the lowest current density of 1.0 mA cm⁻², nearly met the maximum allowed limit for manganese concentration by Ecuadorian regulation, which is 0.40 mg L⁻¹ Mn.

Therefore, to ensure the effective operation of the electrocoagulation system, it is crucial to maintain specific conditions: a pH of approximately 8.5, an operating time of 80 min, a current density of 1.0 mA cm⁻², and a lime dose of 75 mg L⁻¹. These carefully controlled conditions enable the simultaneous removal of hardness (37.6%), sulfate concentrations (14.7%), and manganese (65.3%) in a single reactor. As a result, electrical conductivity is reduced by 15.0%, leading to a residual content of 1501 ± 6 μS cm⁻¹. It is worth noting that these efficiencies meet the criteria set for drinking water quality, ensuring the production of safe and compliant water.

The operation of the bench lab reactor under these conditions requires an energy input of approximately 0.06 kWh m⁻³. A sustainable energy solution can be implemented to meet the daily water production demand of the San Cristobal treatment facility (~200 m³ day⁻¹), which amounts to approximately 115 kW. This involves utilizing around 75 solar photovoltaic panels, each with a capacity of 415 W, and a solar inverter of approximately 26 kW to power the electrocoagulation system. By adopting this approach, not only would the water quality requirements of the community be met, but it would also significantly reduce the carbon footprint associated with drinking water production.

4. Conclusion

The present study systematically evaluated the effectiveness of a laboratory-scale batch electrocoagulation system in treating groundwater from the San Cristobal water treatment plant. The study successfully reduced hardness, sulfate, and manganese concentrations by optimizing crucial operational parameters, including initial pH, operating time, current density, and lime addition. The achieved removal efficiencies were 37.6%, 14.7%, and 65.3%, respectively, meeting the sanitary thresholds established by local water quality regulators.

The results of this study introduce economic implications for the implementation of an electrocoagulation system in vulnerable communities where water contains hardness species (i.e., calcium, magnesium, and sulfates) and manganese. The pH of the solution was found to play a critical role in the electrocoagulation process. Maintaining a solution pH of around 8.5 exhibited superior efficacy in removing hardness and sulfate species compared to acidic (pH ~2.5) or neutral (pH ~7.5) solutions. This result is attributed to the high adsorption properties of the iron flocs generated under basic conditions. Therefore, maintaining a pH level of approximately 8.5 minimizes the cost associated with pH adjustment for drinking water purposes and ensures a more efficient reduction of contaminants in treated water.

Furthermore, the study highlighted the advantage of optimizing the

Table 1

Increase the operating cost as a function of the current density to remove contaminants found in other studies.

Contaminant	Current density	Increase in operating cost	Reference
Calcium hardness and turbidity	From 4.0 mA cm ⁻² to 7.0 mA cm ⁻²	from 1.5 USD to 2.5 USD per m ³	[33]
Fluoride	From 8.3 mA cm ⁻² to 33.3 mA cm ⁻²	from 0.5 USD to 1.5 USD per m ³	[102]
Nitrate	From 6.0 mA cm ⁻² to 9.0 mA cm ⁻²	54 USD per kg of nitrate removed	[103]

operating time and the current density. It was found that high operating time and current density values are not always optimal or able to achieve the maximum limits set in drinking water quality regulations. Careful selection of these conditions ensures effective removal of contaminants such as hardness, sulfate, and manganese, resulting in a notable reduction in energy requirements. This enables the application of electrocoagulation at a larger scale in economically challenged communities. Additionally, integrating cleaner alternative energy sources, such as photovoltaic solar power, could economically meet the long-term energy consumption of the electrocoagulation treatment system. Selecting optimal electrocoagulation conditions could also improve electrode performance and reduce associated maintenance costs.

On the other hand, traditional processes of lime precipitation and alum coagulation, while effective in removing hardness species, pose significant operational challenges due to their high chemical demand and extensive maintenance protocols, including the generation of byproducts such as sludge. These challenges can be particularly problematic for treatment plants serving vulnerable communities without access to government funding for chemical additives, quality monitoring facilities and equipment, and facing difficulties in hiring trained operators. Additionally, conventional chemical precipitation processes may not efficiently address the removal of sulfate and manganese.

In summary, electrocoagulation has proven to be an effective technology for water treatment, enabling the removal of hardness, sulfate, and manganese from drinking water. However, further studies are strongly recommended to optimize operating conditions based on the physicochemical characteristics of water catchment sources and to explore the potential deployment of electrocoagulation in large-scale applications in rural water treatment plants. Addressing these areas of improvement will allow electrocoagulation to contribute significantly to sustainable and efficient water treatment practices.

Funding

This work was supported by the Escuela Superior Politecnica del Litoral ESPOL Polytechnic University, and the Faculty of Engineering in Earth Sciences, project grant [FICT-9-2023].

Declaration of competing interest

The authors declare that they have no known competing financial interests or personal relationships that could have appeared to influence the work reported in this paper.

Data availability

Data will be made available on request.

Acknowledgments

The authors warmly thank Diego Enrique Asanza Moreira and Cristian Alejandro Aguilar Aguilar for their support in the experimentation. This work was performed under the framework of the project Design and Application of Advanced Technologies for Water Treatment, FICT-9-2023.

References

- [1] A. Prüss-Üstün, R. Bos, F. Gore, J. Bartram, *World Health Organization, Safe Water, Better Health : Costs, Benefits and Sustainability of Interventions to Protect and Promote Health*, Geneva, 2008.
- [2] M. Sauvant, D. Pepin, Drinking water and cardiovascular disease, *Food Chem. Toxicol.* 40 (2002) 13–1325, [https://doi.org/10.1016/s0278-6915\(02\)00081-9](https://doi.org/10.1016/s0278-6915(02)00081-9).
- [3] A.M. Dietrich, G.A. Burlingame, Critical review and rethinking of USEPA secondary standards for maintaining organoleptic quality of drinking water, *American Chemical Society, Environ. Sci. Technol.* 49 (2) (Jan. 20, 2015) 708–720, <https://doi.org/10.1021/es504403t>.

- [4] WHO, *Guidelines for Drinking-Water Quality, fourth edition incorporating the first addendum*, Geneva, 2017.
- [5] D.S. Harischandra, et al., Manganese-induced neurotoxicity: new insights into the triad of protein misfolding, mitochondrial impairment, and neuroinflammation, *Frontiers Media S.A. Front. Neurosci.* 13 (JUN) (2019) <https://doi.org/10.3389/fnins.2019.00654>.
- [6] R.C. Balachandran, et al., Brain manganese and the balance between essential roles and neurotoxicity, *American Society for Biochemistry and Molecular Biology Inc. J. Biol. Chem.* 295 (19) (May 08, 2020) 6312–6329, <https://doi.org/10.1074/jbc.REV119.009453>.
- [7] M.A. Jeuland, D.E. Fuente, S. Ozdemir, M.C. Allaire, D. Whittington, The long-term dynamics of mortality benefits from improved water and sanitation in less developed countries, *PLoS One* 8 (10) (Oct. 2013), <https://doi.org/10.1371/journal.pone.0074804>.
- [8] R. Kumar, et al., Emerging technologies for arsenic removal from drinking water in rural and peri-urban areas: methods, experience from, and options for Latin America, *Sci. Total Environ.* 694 (Dec. 2019), <https://doi.org/10.1016/j.scitotenv.2019.07.233>.
- [9] J.I. Mendez-Ruiz, M.B. Barcia-Carreño, L.J. Mejía-Bustamante, Á.K. Cornejo-Pozo, C.A. Salas-Vázquez, P.E. Valverde-Armas, Assessment of the performance of a water treatment plant in Ecuador: hydraulic resizing of the treatment units, *Sustainability* 15 (no. 2) (2023), <https://doi.org/10.3390/su15021235>.
- [10] S.E.H. Comstock, T.H. Boyer, Combined magnetic ion exchange and cation exchange for removal of DOC and hardness, *Chem. Eng. J.* 241 (Apr. 2014) 366–375, <https://doi.org/10.1016/j.cej.2013.10.073>.
- [11] R.D.R. Silva, R.T. Rodrigues, A.C. Azevedo, J. Rubio, Calcium and magnesium ion removal from water feeding a steam generator by chemical precipitation and flotation with micro and nanobubbles, *Environ. Technol.* 41 (17) (Jul. 2020) 2210–2218, <https://doi.org/10.1080/09593330.2018.1558288>.
- [12] L. K. Wang, D. A. Vaccari, Y. Li, and N. K. Shammam, "Chemical Precipitation.
- [13] D. Clifford, S. Subramanian, T.J. So, Removing dissolved inorganic contaminants from water, *Environ. Sci. Technol.* 20 (1986).
- [14] D. Qu, J. Wang, L. Wang, D. Hou, Z. Luan, B. Wang, Integration of accelerated precipitation softening with membrane distillation for high-recovery desalination of primary reverse osmosis concentrate, *Sep. Purif. Technol.* 67 (1) (May 2009) 21–25, <https://doi.org/10.1016/j.seppur.2009.02.021>.
- [15] W. Liu, L. Sun, S. Tao, Removal of Ca²⁺, Mg²⁺, Ba²⁺ and Sr²⁺ from shale gas flowback water from the Sichuan Basin in China by chemical softening under the guidance of OLI Stream Analyzer: precipitation behaviors and optimization study, *Water Sci. Technol.* 82 (1) (Jul. 2020) 194–206, <https://doi.org/10.2166/wst.2020.355>.
- [16] M.Y.A. Mollah, P. Morkovsky, J.A.G. Gomes, M. Kesmez, J. Parga, D.L. Cocke, Fundamentals, present and future perspectives of electrocoagulation, *J. Hazard Mater.* 114 (1–3) (Oct. 2004) 199–210, <https://doi.org/10.1016/j.jhazmat.2004.08.009>.
- [17] D.T. Moussa, M.H. El-Naas, M. Nasser, M.J. Al-Marri, A comprehensive review of electrocoagulation for water treatment: potentials and challenges, *Academic Press, J. Environ. Manag.* 186 (Jan. 15, 2017) 24–41, <https://doi.org/10.1016/j.jenvman.2016.10.032>.
- [18] M.M. Emamjomeh, M. Sivakumar, Review of pollutants removed by electrocoagulation and electrocoagulation/flotation processes, *J. Environ. Manag.* 90 (5) (Apr. 2009) 1663–1679, <https://doi.org/10.1016/j.jenvman.2008.12.011>.
- [19] M. Yousuf, A. Mollah, R. Schennach, J.R. Parga, D.L. Cocke, *Electrocoagulation (EC)-science and Applications*, 2001.
- [20] J. Rodriguez, S. Stojić, G. Krause, B. Friedrich, Feasibility assessment of electrocoagulation towards a new sustainable wastewater treatment, *Environ. Sci. Pollut. Control Ser.* 14 (7) (Nov. 2007) 477–482, <https://doi.org/10.1065/espr2007.05.424>.
- [21] M. Bayramoglu, M. Eyvaz, M. Kobya, Treatment of the textile wastewater by electrocoagulation. Economical evaluation, *Chem. Eng. J.* 128 (2–3) (Apr. 2007) 155–161, <https://doi.org/10.1016/j.cej.2006.10.008>.
- [22] B. Khaled, B. Wided, H. Béchir, E. Elimame, L. Mouna, T. Zied, Investigation of electrocoagulation reactor design parameters effect on the removal of cadmium from synthetic and phosphate industrial wastewater, *Arab. J. Chem.* 12 (8) (Dec. 2019) 1848–1859, <https://doi.org/10.1016/j.arabjc.2014.12.012>.
- [23] F.R. Espinoza-Quinones, et al., Pollutant removal from tannery effluent by electrocoagulation, *Chem. Eng. J.* 151 (1–3) (Aug. 2009) 59–65, <https://doi.org/10.1016/j.cej.2009.01.043>.
- [24] D. Marmanis, C. Emmanouil, J.G. Fantidis, A. Thysiadou, K. Marmani, Description of a Fe/Al electrocoagulation method powered by a photovoltaic system, for the (Pre-)Treatment of municipal wastewater of a small community in northern Greece, *Sustainability* 14 (7) (Apr. 2022), <https://doi.org/10.3390/su14074323>.
- [25] C.J. Nawarkar, V.D. Salkar, Solar powered Electrocoagulation system for municipal wastewater treatment, *Fuel* 237 (Feb. 2019) 222–226, <https://doi.org/10.1016/j.fuel.2018.09.140>.
- [26] N.A. Rahman, et al., Development of solar power system for Sarawak peat water continuous electrocoagulation treatment process, *IOP Conf. Ser. Mater. Sci. Eng.* 1101 (1) (Mar. 2021), 012039, <https://doi.org/10.1088/1757-899x/1101/1/012039>.
- [27] S. Yamba, R.M. Moutloali, N. Mabuba, Corrugated iron sheets for electrocoagulation of sulphate ions in industrial effluents, *Case Studies in Chemical and Environmental Engineering* 2 (March) (2020), 100061, <https://doi.org/10.1016/j.cscee.2020.100061>.

- [28] N.G. Yasri, et al., Investigation of electrode passivation during electrocoagulation treatment with aluminum electrodes for high silica content produced water, *Water Sci. Technol.* 85 (3) (Feb. 2022) 925–942, <https://doi.org/10.2166/wst.2022.012>.
- [29] M.A. Mamelkina, R. Tuunila, M. Sillanpää, A. Häkkinen, Systematic study on sulfate removal from mining waters by electrocoagulation, *Sep. Purif. Technol.* 216 (October 2018) (2019) 43–50, <https://doi.org/10.1016/j.seppur.2019.01.056>.
- [30] J.U. Halpegama, et al., Concurrent removal of hardness and fluoride in water by monopolar electrocoagulation, *J. Environ. Chem. Eng.* 9 (5) (2021), 106105, <https://doi.org/10.1016/j.jece.2021.106105>.
- [31] M. Mahmood, N. Yasri, B. Fuladpanjeh-Hojaghan, E.P.L. Roberts, Influence of operating conditions on the removal of silica and hardness by continuous electrocoagulation, *J. Environ. Chem. Eng.* 10 (6) (2022), 108899, <https://doi.org/10.1016/j.jece.2022.108899>.
- [32] M. Salam, R.K. Purnama, B. Latifah, Study of Fe, Ca, and Mg removal using electrocoagulation method from wastewater integrated canal, in: *IOP Conference Series: Earth and Environmental Science*, Institute of Physics, Apr. 2022, <https://doi.org/10.1088/1755-1315/1017/1/012025>.
- [33] P. Sefatjoo, M.R. Alavi Moghaddam, A.R. Mehrabadi, Evaluating electrocoagulation pretreatment prior to reverse osmosis system for simultaneous scaling and colloidal fouling mitigation: application of RSM in performance and cost optimization, *J. Water Process Eng.* 35 (July 2019) (2020), 101201, <https://doi.org/10.1016/j.jwpe.2020.101201>.
- [34] M. Malakootian, H.J. Mansoorian, M. Moosazadeh, Performance evaluation of electrocoagulation process using iron-rod electrodes for removing hardness from drinking water, *Desalination* 255 (1–3) (2010) 67–71, <https://doi.org/10.1016/j.desal.2010.01.015>.
- [35] S. Zhao, G. Huang, G. Cheng, Y. Wang, H. Fu, Hardness, COD and turbidity removals from produced water by electrocoagulation pretreatment prior to reverse osmosis membranes, *Desalination* 344 (2014) 454–462, <https://doi.org/10.1016/j.desal.2014.04.014>.
- [36] J.T. Medina-Collana, G.E. Reyna-Mendoza, J.A. Montaña-Pisfil, J.A. Rosales-Huamani, E.J. Franco-Gonzales, X. Córdoba García, Evaluation of the performance of the electrocoagulation process for the removal of water hardness, *Sustainability* 15 (1) (Jan. 2023), <https://doi.org/10.3390/su15010590>.
- [37] Ö. Hanay, H. Hasar, Effect of anions on removing Cu²⁺, Mn²⁺ and Zn²⁺ in electrocoagulation process using aluminum electrodes, *J. Hazard Mater.* 189 (1–2) (2011) 572–576, <https://doi.org/10.1016/j.jhazmat.2011.02.073>.
- [38] B. Al Aji, Y. Yavuz, A.S. Kopardal, Electrocoagulation of heavy metals containing model wastewater using monopolar iron electrodes, *Sep. Purif. Technol.* 86 (Feb. 2012) 248–254, <https://doi.org/10.1016/j.seppur.2011.11.011>.
- [39] E. Gatsios, J.N. Hahladakis, E. Gidararakos, Optimization of electrocoagulation (EC) process for the purification of a real industrial wastewater from toxic metals, *J. Environ. Manag.* 154 (May 2015) 117–127, <https://doi.org/10.1016/j.jenvman.2015.02.018>.
- [40] A. Shafaei, M. Rezaeie, M. Arami, M. Nikazar, Removal of Mn²⁺ ions from synthetic wastewater by electrocoagulation process, *Desalination* 260 (1–3) (2010) 23–28, <https://doi.org/10.1016/j.desal.2010.05.006>.
- [41] A. Shafaei, M. Rezaie, M. Nikazar, Evaluation of Mn²⁺ and Co²⁺ removal by electrocoagulation: a case study, *Chem. Eng. Process: Process Intensif.* 50 (11–12) (2011) 1115–1121, <https://doi.org/10.1016/j.ccep.2011.10.003>.
- [42] N. Mohd Yussuf, et al., Biochar-coated aluminium electrodes for Cr, Mn and Fe removal in electrochemical treatment for polluted river water remediation, *IOP Conf. Ser. Mater. Sci. Eng.* 555 (1) (2019), <https://doi.org/10.1088/1757-899X/555/1/012011>.
- [43] P. López, A. Harnisth, Electrocoagulación de aguas residuales de la industria láctea, *Enfoque UTE* 7 (1) (Mar. 2016) 13–21, <https://doi.org/10.29019/enfoqueute.v7n1.84>.
- [44] A. Guamán, M. Guamán, C. Álvarez, Aplicación del principio de electrocoagulación en el tratamiento del agua residual textil [Online]. Available: DELOS Desarrollo Local Sostenible, Málaga, Jun. 2016 www.eumed.net/rev/delos/26.
- [45] INEC, Resultados de Censo de población y vivienda 1992-2021. Diseminación de datos, Instituto de Estadísticas y Censo, 2022.
- [46] INEN, NTE INEN 2169. *Water Sampling, Conservation, and Transportation Procedures*, 2013, p. 26.
- [47] HACH, Method 8222, Calcium hardness, 2016.
- [48] HACH, Method 8226, Total hardness, 2021.
- [49] HACH, Method 8221, Alkalinity, 2017.
- [50] HACH, Method 8051: Sulfate, 2019.
- [51] HACH, Method 8113: Chloride, 2018.
- [52] O. Korchuganova, I. Afonina, P. Prygorodov, V. Mokhonko, K. Kanarova, Utilization of lime-softening sludge to obtain calcium nitrate, *E. Eur. J. Enterprise Technol.* 4 (10–94) (2018) 46–53, <https://doi.org/10.15587/1729-4061.2018.141007>.
- [53] S.E.H. Comstock, T.H. Boyer, K.C. Graf, Treatment of nanofiltration and reverse osmosis concentrates: comparison of precipitative softening, coagulation, and anion exchange, *Water Res.* 45 (16) (2011) 4855–4865, <https://doi.org/10.1016/j.watres.2011.06.035>.
- [54] J. Van Leeuwen, D.J. White, R.J. Baker, C. Jones, Reuse of water treatment residuals from lime softening, Part I: applications for the reuse of lime sludge from water softening, *Land Contam. Reclam.* 18 (4) (2010) 393–415, <https://doi.org/10.2462/09670513.1012>.
- [55] A.R. Prazeres, J. Rivas, Ú. Paulo, F. Ruas, F. Carvalho, Sustainable treatment of different high-strength cheese whey wastewaters: an innovative approach for atmospheric CO₂ mitigation and fertilizer production, *Environ. Sci. Pollut. Control Ser.* 23 (13) (2016) 13062–13075, <https://doi.org/10.1007/s11356-016-6429-3>.
- [56] S. Chen, T. Chang, C. Lin, Silica pretreatment for a RO brackish water source with high magnesium, *Water Sci. Technol. Water Supply* 6 (4) (2006) 179–187, <https://doi.org/10.2166/ws.2006.792>.
- [57] L. Madeira, F. Carvalho, A. Almeida, M. Ribau Teixeira, Optimization of atmospheric carbonation in the integrated treatment immediate one-step lime precipitation and atmospheric carbonation. The case study of slaughterhouse effluents, *Results in Engineering* 17 (November 2022) (2023), <https://doi.org/10.1016/j.rineng.2022.100807>.
- [58] S. Renou, S. Poulain, J.G. Givaudan, P. Moulin, Amelioration of ultrafiltration process by lime treatment: case of landfill leachate, *Desalination* 249 (1) (2009) 72–82, <https://doi.org/10.1016/j.desal.2008.09.007>.
- [59] R. Ordóñez, A. Moral, D. Hermosilla, ángeles Blanco, Combining coagulation, softening and flocculation to dispose reverse osmosis retentates, *J. Ind. Eng. Chem.* 18 (3) (2012) 926–933, <https://doi.org/10.1016/j.jiec.2011.08.004>.
- [60] A. Zayen, G. Schories, S. Sayadi, Incorporation of an anaerobic digestion step in a multistage treatment system for sanitary landfill leachate, *Waste Manag.* 53 (2016) 32–39, <https://doi.org/10.1016/j.wasman.2016.04.030>.
- [61] M. Yan, D. Wang, J. Ni, J. Qu, Y. Yan, C.W.K. Chow, Effect of polyaluminum chloride on enhanced softening for the typical organic-polluted high hardness North-China surface waters, *Sep. Purif. Technol.* 62 (2) (2008) 401–406, <https://doi.org/10.1016/j.seppur.2008.02.014>.
- [62] M.A. Yukselen, J. Gregory, The effect of rapid mixing on the break-up and re-formation of flocs, *J. Chem. Technol. Biotechnol.* 79 (7) (2004) 782–788, <https://doi.org/10.1002/jctb.1056>.
- [63] Q.H. Malik, Performance of alum and assorted coagulants in turbidity removal of muddy water, *Appl. Water Sci.* 8 (1) (2018) 1–4, <https://doi.org/10.1007/s13201-018-0662-5>.
- [64] D. Gheraout, et al., Combining lime softening with alum coagulation for hard Ghrif dam water conventional treatment, *International Journal of Advanced and Applied Sciences* 5 (5) (2018) 61–70, <https://doi.org/10.21833/ijaa.2018.05.008>.
- [65] N. Bouchahm, L. Hecini, W. Kherifi, Softening of groundwater in the eastern region of the northern Algeria Sahara: case of the Biskra region, *J. Water Sci.* 29 (1) (2016) 37–48, <https://doi.org/10.7202/1035715ar>.
- [66] J. Sánchez Rubal, J.A. Cortacans Torre, I. Del Castillo González, Influence of temperature, agitation, sludge concentration and solids retention time on primary sludge fermentation, *Int. J. Chem. Eng.* 2012 (2012), <https://doi.org/10.1155/2012/861467>.
- [67] N.A. Oladoja, Y.D. Aliu, Snail shell as coagulant aid in the alum precipitation of malachite green from aqua system, *J. Hazard Mater.* 164 (2–3) (2009) 1496–1502, <https://doi.org/10.1016/j.jhazmat.2008.09.114>.
- [68] S.J. Randtke, C.E. Thiel, M.Y. Liao, C.N. Yamaya, Removing soluble organic contaminants by lime-softening, *J. Am. Water Works Assoc.* 74 (4) (1982) 192–202, <https://doi.org/10.1002/j.1551-8833.1982.tb04888.x>.
- [69] C.L. Yang, Electrochemical coagulation for oily water demulsification, *Sep. Purif. Technol.* 54 (3) (2007) 388–395, <https://doi.org/10.1016/j.seppur.2006.10.019>.
- [70] M. Kobya, O.T. Can, M. Bayramoglu, Treatment of textile wastewaters by electrocoagulation using iron and aluminum electrodes, *J. Hazard Mater.* 100 (1–3) (2003) 163–178, [https://doi.org/10.1016/S0304-3894\(03\)00102-X](https://doi.org/10.1016/S0304-3894(03)00102-X).
- [71] M. Kobya, E. Demirbas, F. Ulu, Evaluation of operating parameters with respect to charge loading on the removal efficiency of arsenic from potable water by electrocoagulation, *J. Environ. Chem. Eng.* 4 (2) (2016) 1484–1494, <https://doi.org/10.1016/j.jece.2016.02.016>.
- [72] R. Katal, H. Pahlavanzadeh, Influence of different combinations of aluminum and iron electrode on electrocoagulation efficiency: application to the treatment of paper mill wastewater, *Desalination* 265 (1–3) (2011) 199–205, <https://doi.org/10.1016/j.desal.2010.07.052>.
- [73] C. Hu, S. Wang, J. Sun, H. Liu, J. Qu, An effective method for improving electrocoagulation process: optimization of Al13 polymer formation, *Colloids Surf. A Physicochem. Eng. Asp.* 489 (2016) 234–240, <https://doi.org/10.1016/j.colsurfa.2015.10.063>.
- [74] X. Chen, G. Chen, P.L. Yue, Separation of pollutants from restaurant wastewater by electrocoagulation, *Sep. Purif. Technol.* 19 (1–2) (2000) 65–76, [https://doi.org/10.1016/S1383-5866\(99\)00072-6](https://doi.org/10.1016/S1383-5866(99)00072-6).
- [75] L. Xu, et al., Simultaneous removal of cadmium, zinc and manganese using electrocoagulation: influence of operating parameters and electrolyte nature, *J. Environ. Manag.* 204 (2017) 394–403, <https://doi.org/10.1016/j.jenvman.2017.09.020>.
- [76] A.A. Al-Raad, M.M. Hanafiah, Sulfate (SO₄²⁻) removal by electrocoagulation process under combined electrical connection of electrodes, *IOP Conf. Ser. Earth Environ. Sci.* 880 (1) (2021), <https://doi.org/10.1088/1755-1315/880/1/012033>.
- [77] S.D. Mengesha, A. Weldetsinae, K. Tesfaye, G. Taye, Organoleptic and palatability properties of drinking water sources and its health implications in Ethiopia: a retrospective study during 2010–2016, *Environmental Health Engineering and Management* 5 (4) (Oct. 2018) 221–229, <https://doi.org/10.15171/EHEM.2018.30>.
- [78] J. Hofman, J.P. Van Der Hoek, M. Nederlof, M. Groenendijk, “Twenty years of experience with centralised softening in The Netherlands: water quality, environmental benefits, and costs;”, *Water* 21 (FEB) (Feb. 2007) 21–24.
- [79] INEN, NTE INEN 1108. *Drinking Water, Quality Requirements*, 2011, p. 9.
- [80] United States Environmental Protection Agency, 2012 Edition of the Drinking Water Standards and Health Advisories, 2012.

- [81] J.C. Egbueri, A multi-model study for understanding the contamination mechanisms, toxicity and health risks of hardness, sulfate, and nitrate in natural water resources, *Environ. Sci. Pollut. Control Ser.* 30 (22) (2023) 61626–61658, <https://doi.org/10.1007/s11356-023-26396-5>.
- [82] K. Ljung, F. Maley, A. Cook, P. Weinstein, Acid sulfate soils and human health-A Millennium Ecosystem Assessment, *Environ. Int.* 35 (8. Pergamon) (Nov. 01, 2009) 1234–1242, <https://doi.org/10.1016/j.envint.2009.07.002>.
- [83] A.E. Griffin, Significance and removal of manganese in water supplies, *J. Am. Water Works Assoc.* 52 (10) (Oct. 1960) 1326–1334, <https://doi.org/10.1002/J.1551-8833.1960.TB00599.X>.
- [84] M. Catalán-Vázquez, A. Schilman, H. Riojas-Rodríguez, Perceived health risks of manganese in the molango mining district, Mexico, *Risk Anal.* 30 (4) (2010) 619–634, <https://doi.org/10.1111/j.1539-6924.2010.01377.x>.
- [85] S. Xiao, et al., The association between manganese exposure with cardiovascular disease in older adults: NHANES 2011–2018, *Journal of Environmental Science and Health, Part A* 56 (11) (Sep. 2021) 1221–1227, <https://doi.org/10.1080/10934529.2021.1973823>.
- [86] X. Ba, et al., An integrated electrolysis-microfiltration-ion exchange closed-loop system for effective water softening without chemicals input and spent regenerant discharge, *Desalination* 553 (May 2023), <https://doi.org/10.1016/J.DESAL.2023.116481>.
- [87] WHO, Guidelines for Drinking-Water Quality: Fourth Edition Incorporating the First and Second Addenda, vol. 4, World Health Organization, 2011, p. 608.
- [88] S.A. Imran, J.D. Dietz, G. Mutoti, W. Xiao, J.S. Taylor, V. Desai, Optimizing source water blends for corrosion and residual control in distribution systems, *J. Am. Water Works Assoc.* 98 (5) (2006) 107–115, <https://doi.org/10.1002/j.1551-8833.2006.tb07664.x>.
- [89] B. Palahouane, N. Drouiche, S. Aoudj, K. Bensadok, Cost-effective electrocoagulation process for the remediation of fluoride from pretreated photovoltaic wastewater, *J. Ind. Eng. Chem.* 22 (2015) 127–131, <https://doi.org/10.1016/j.jiec.2014.06.033>.
- [90] I. Kabdaşlı, I. Arslan-Alaton, T. Ölmez-Hancı, O. Tünay, Electrocoagulation applications for industrial wastewaters: a critical review, *Environmental Technology Reviews* 1 (1) (2012) 2–45, <https://doi.org/10.1080/21622515.2012.715390>.
- [91] C.A. Martínez-Huitle, Environment-friendly electrochemical processes, *Materials* 14 (6) (2021) 10–12, <https://doi.org/10.3390/ma14061548>.
- [92] W.L. Chou, C.T. Wang, K.Y. Huang, Effect of operating parameters on indium (III) ion removal by iron electrocoagulation and evaluation of specific energy consumption, *J. Hazard Mater.* 167 (1–3) (2009) 467–474, <https://doi.org/10.1016/j.jhazmat.2009.01.008>.
- [93] G. Chen, Electrochemical technologies in wastewater treatment, *Sep. Purif. Technol.* 38 (1) (2004) 11–41, <https://doi.org/10.1016/j.seppur.2003.10.006>.
- [94] M. Muruganathan, G. Bhaskar Raju, S. Prabhakar, Removal of sulfide, sulfate and sulfite ions by electro coagulation, *J. Hazard Mater.* 109 (1–3) (2004) 37–44, <https://doi.org/10.1016/j.jhazmat.2003.12.009>.
- [95] E. Nariyan, C. Wolkersdorfer, M. Sillanpää, Sulfate removal from acid mine water from the deepest active European mine by precipitation and various electrocoagulation configurations, *J. Environ. Manag.* 227 (September) (2018) 162–171, <https://doi.org/10.1016/j.jenvman.2018.08.095>.
- [96] S. Radić, V. Vujčić, Ž. Cvetković, P. Cvjetko, V. Oreščanin, The efficiency of combined CaO/electrochemical treatment in removal of acid mine drainage induced toxicity and genotoxicity, *Sci. Total Environ.* 466–467 (2014) 84–89, <https://doi.org/10.1016/j.scitotenv.2013.07.011>.
- [97] A. Kumar, P.V. Nidheesh, M. Suresh Kumar, Composite wastewater treatment by aerated electrocoagulation and modified peroxi-coagulation processes, *Chemosphere* 205 (2018) 587–593, <https://doi.org/10.1016/j.chemosphere.2018.04.141>.
- [98] D. Lakshmanan, D.A. Clifford, G. Samanta, Ferrous and ferric ion generation during iron electrocoagulation, *Environ. Sci. Technol.* 43 (10) (2009) 3853–3859, <https://doi.org/10.1021/es803666g>.
- [99] H.A. Moreno, et al., Electrochemical generation of green rust using electrocoagulation, *ECS Trans.* 3 (18) (2007) 67, <https://doi.org/10.1149/1.2753225>.
- [100] P. Del Ángel, G. Carreño, J.L. Nava, M.T. Martínez, J. Ortiz, Removal of arsenic and sulfates from an abandoned mine drainage by electrocoagulation. Influence of hydrodynamic and current density, *Int. J. Electrochem. Sci.* 9 (2) (2014) 710–719.
- [101] S. Farhadi, B. Aminzadeh, A. Torabian, V. Khatibikamal, M. Alizadeh Fard, Comparison of COD removal from pharmaceutical wastewater by electrocoagulation, photoelectrocoagulation, peroxi-electrocoagulation and peroxi-photoelectrocoagulation processes, *J. Hazard Mater.* 219–220 (Jun. 2012) 35–42, <https://doi.org/10.1016/j.jhazmat.2012.03.013>.
- [102] M. Behbahani, M.R.A. Moghaddam, M. Arami, Techno-economical evaluation of fluoride removal by electrocoagulation process: optimization through response surface methodology, *Desalination* 271 (1–3) (2011) 209–218, <https://doi.org/10.1016/j.desal.2010.12.033>.
- [103] E. Karamati-Niaragh, M.R. Alavi Moghaddam, M.M. Emamjomeh, E. Nazlabadi, Evaluation of direct and alternating current on nitrate removal using a continuous electrocoagulation process: economical and environmental approaches through RSM, *J. Environ. Manag.* 230 (May 2018) (2019) 245–254, <https://doi.org/10.1016/j.jenvman.2018.09.091>.
- [104] N. Adhoum, L. Monser, N. Bellakhal, J.E. Belgaied, Treatment of electroplating wastewater containing Cu²⁺, Zn²⁺ and Cr(VI) by electrocoagulation, *J. Hazard Mater.* 112 (3) (2004) 207–213, <https://doi.org/10.1016/j.jhazmat.2004.04.018>.
- [105] R.S. Alkizwini, et al., Optimization of electrochemical removal of metal pollution from aqueous solution, *IOP Conf. Ser. Mater. Sci. Eng.* 1058 (1) (2021), 012022, <https://doi.org/10.1088/1757-899x/1058/1/012022>.